An Overview of Determination of Young's modulus by AFM in Various Fields

Maryam Daraee,[1*] Sedigheh Sadegh Hassani[2,3,**] and Somayeh Jalilzadeh Azar[3,4]

[1]Nano Compound Seman Dara Company, Mahdishahr, Semnan, Iran

[2] Catalysis Research Division, Research Institute of Petroleum Industry (RIPI), Tehran, Iran

[3] Iran Laboratory Network, SPM Experts work group

[4] M.Sc. Microbiology, Chemistry & Chemical Engineering Research Center of Iran, Tehran, Iran

Corresponding author: * m20.daraee@gmail.com

**nsadeghhassani@yahoo.co.uk

Abstract

The Atomic Force Microscope (AFM) is a powerful tool for studying the properties and structures of materials at the nanometer scale. Unlike most surface analysis methods, it has no restrictions on surface types or their environment. This versatility allows AFM to investigate a wide range of materials, including conductive, insulating, soft, hard, cohesive, powdered, biological, organic, and inorganic. As such, it finds applications in diverse scientific fields such as chemistry, surface chemistry, polymer science, physics, molecular engineering, semiconductor science, biology, and medicine. Beyond its ability to image surfaces, AFM can also measure mechanical properties like Young's modulus. Young's modulus, also known as the modulus of elasticity (E), is defined as the ratio of stress to strain in the elastic region. This value reflects the stiffness of a material and changes with temperature. This paper explores the application of AFM in measuring Young's modulus across various scientific disciplines.

Keywords: Atomic force microscope; Young's modulus; Force curve; Elasticity; Stress; Strain.

Introduction

Young's modulus as one of the most important mechanical properties of materials is defined as the elastic properties of a solid substance that it undergoing tension or compression in only one direction, which sometimes it nominated as elasticity, it is named after the Thomas Young (one of the 19th century British scientists) [1-2].

The modulus of elasticity is actually the ratio of stress to strain of a substance and it is a constant value for each material. Modulus of elasticity is used as a way to identify different materials. Recently, atomic force microscopy (AFM) as a characterizing technique, has been used to quantitatively determine of surface mechanical properties. The atomic force microscope is a powerful non-destructive tool to imaging the surfaces topography with nanometric resolution. In addition, by AFM some information about friction behavior, thermal properties, and surface elasticity can be obtained that cannot be achieved using other methods. This microscope usually does not require the very high vacuum such as TEM and SEM [3-5]. It can be used to determine the Young's modulus of substrates by study of interaction between the tip and surface [6-9]. Moreover, the mechanical properties of cells or tissues in biological and unbiologic systems can be investigated using AFM.

Young's modulus

Young's modulus as a very important material property describes the elastic properties of a solid under tension or compression in one direction, which shows a solid's stiffness or resistance to elastic deformation under load. The influence of strains on the under-load material leads to displacement of structure.

Young's modulus is the ratio of tensile stress to tensile strain along a line, which stress and strain defined as force per unit area and proportional deformation, respectively. Figure 1 a, b shows the effect of stiffness on the Young's modulus value with change in length, respectively. A uniaxial stress (extension or compression) is given to material with low stiffness (green Fig.1-a) and high stiffness (blue Fig. 1-a) that it can be cause their deformation [10-11].

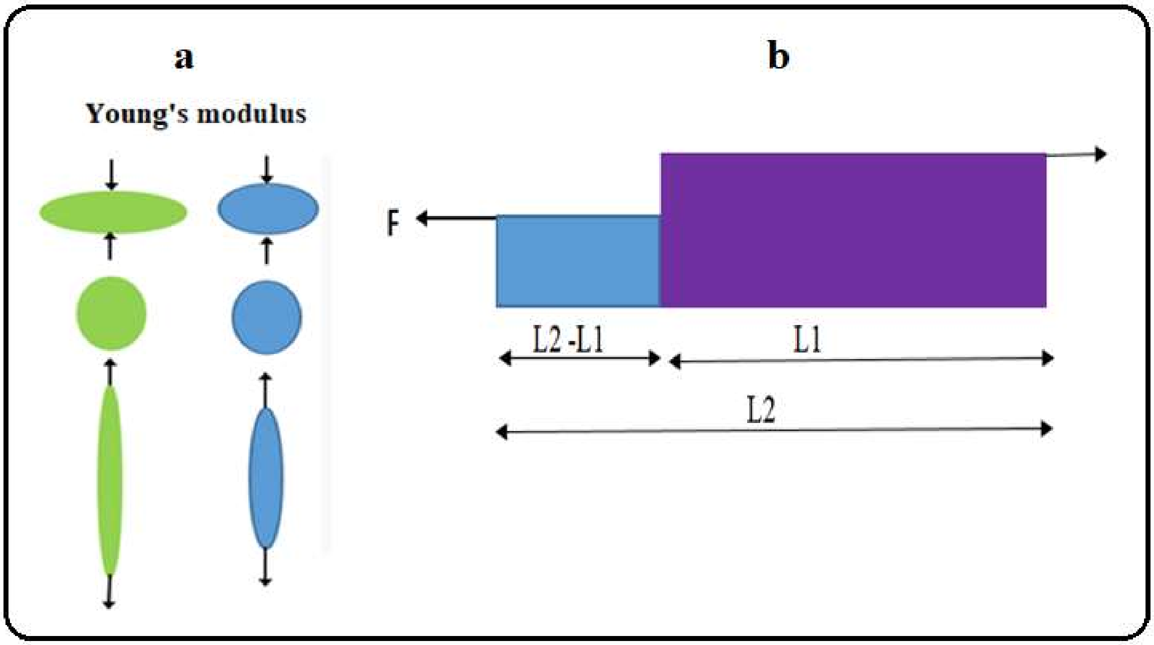

Figure 1: Effect of stiffness on Young's modulus value.

By compressing or extending of materials, the elastic deformation occurs that will return to their original shape by removing the load. Flexible materials or elastic solids show a low Young's modulus value and a stiff materials or inelastic solids indicate a high Young's modulus.

The equation for Young's modulus is:

$E = \text{stress/strain} = \sigma / \varepsilon = (F/A) / (\Delta L/L_1) = FL_1 / A\Delta L$

Where E, σ, and ε are Young's modulus (Pa), the uniaxial stress and the strain, F defined as the force of compression or extension, A is the cross-sectional surface area perpendicular to the applied force, Δ L and L are the change in length (negative under compression; positive when stretched) and the original length, respectively. L_2 is new length (Fig. 1-b).

Atomic Force Microscope

Atomic Force Microscope can be used to measure several properties including surface morphology, adhesion and friction forces, elasticity, magnetic properties, distribution of electric charges and electrical polarity of different points. These capabilities are used to evaluate properties such as roughness, uniformity, adhesion, corrosion, friction, size and so on, which applied in various fields and industries including chemistry, physics, materials and metallurgy, polymer engineering, biology, medicine, and so on [12-16].

The AFM works by bringing the cantilever tip close to the sample surface. A laser beam reflects off the backside of the cantilever, and its position is recorded by a photodiode. Any attractive or repulsive forces between the tip and the surface cause the cantilever to bend, changing the direction of the reflected beam. The detector measures the amount of this deflection, allowing us to generate a topographic map of the sample surface with nanometer-scale resolution in the X and Y directions and angstrom-level resolution in the Z direction [17-19].

Using the AFM, making nanometer changes in the sample surfaces by both mechanical and chemical methods is possible. Among the AFM capabilities, making nano-indentation is also important, which is valuable capability for Young's modulus investigation. AFM would able to monitor the surface via in situ imaging of the indentation without switching equipment [20]. Several factors influence the calculation of Young's modulus using AFM, including temperature changes, cantilever shape and geometry, and beam shape. This technique can be applied to diverse materials like rubber, polymers, metals, glasses, alloys, carbon nanotubes, graphene, and diamond. Generally, solids possess high Young's moduli, while elastomers have low values.

The calculation involves determining the slope of the linear portion of the stress-strain curve. For simplicity, the Hertz model is a recommended approach to extract necessary quantities. This requires obtaining the cantilever tip's dimensions (length, width, thickness, and radius) using calibration samples and SEM images [20].

The cantilever's response is recorded after introducing the modulation signal to the sample using the responsive phase and amplitude. Young's modulus can be calculated by phase and amplitude versus driving frequency. Also, it can be obtained from the resonance frequencies between the tip-surface interaction and the Young's modulus, or modulus of elasticity is calculated by determining the force created at the resonance frequency of the sample [21].

Hertz model

In 1881, Heinrich Hertz presented Hertz model, which the tip and the sample are assumed as two spheres by considering elastic deformation with radius R1 and R2, respectively. So, both the interpenetration between surfaces during the indentation process and any F_a acting between the surface and the AFM tip are ignored [20].

Applying this model is only possible if the probe indentation value into the sample surface is much smaller than the tip curvature radius, in order to eliminate the plastic deformations in the sample surface. Finding the contact point between the tip and the sample surface is so important in force F measurement dependent on the indentation value δ [22].

However, the equation in this model is summarized in the following formula:

$$A_c = \pi \left(\frac{RF}{K}\right)^{2/3}$$

R is obtained by incorporating the curvature radius of different materials and K is related to their combined elastic modulus, which is formulated as following:

$$K = \frac{4}{3}\left(\frac{1-\upsilon_i^2}{E_i} + \frac{1-\upsilon^2}{E}\right)^{-1}$$

E is the Young's modulus and ν is the Poisson ratio for the material and the indenter.

Johnson, Kendall and Roberts [23] designed a mechanics model for calculating of A_c, as follows:

$$\gamma = \gamma_1 + \gamma_2 - \gamma_{12}$$

Υ is the work per unit of area that is necessary to separate the tip and surface. Υ_1 and Υ_2 are the surface energies of the sample and surface, Υ_{12} is the interfacial energy. This model is more credible for sticky surfaces and tips with a large R and interaction forces are ignored. According to this model, A_c is formulates as:

$$A_c = \pi \frac{R^{2/3}}{K^{2/3}}\left(F + 3\pi\gamma R + \sqrt{6\pi\gamma RF + (3\pi\gamma R)^2}\right)^{2/3}$$

When the value of Υ tends to zero, the above equation approaches the Hertz model.

Application of AFM in determination of Young's modulus

Atomic force microscopy is a strong tool for studying a wide range of materials at the nanoscale. Using of this microscope, it is possible to study the structural, physical and mechanical properties of materials such as roughness, hardness, Young's modulus, topography and particle size as well as force determination in nano-Newton scale.

It can be applied in in various fields such as chemistry, materials, physics, polymer, Semiconductor and others sciences. Imaging of biomolecules in physiological condition, is one of the capabilities of AFM, which makes this technique widely used in biology and medical, too.

This device also has the ability to nanoindentation investigation and change the particles and sample surfaces [24-28]. This article briefly describes some of the most important uses of the AFM in Young's modulus determination in the various fields.

Application of AFM in the Young's modulus determination in the biological science

Understanding the mechanical properties of biological tissues is crucial for detecting disease states, maintaining tissue homeostasis, and guiding reconstructions. Mesenchymal stromal/stem cells (MSCs) derived from human tissues have demonstrated therapeutic potential in various applications, including bone and tissue formation, repair, reconstruction, and cell therapy. Notably, MSCs are known to be sensitive to mechanical cues such as shear stress and matrix stiffness. Atomic force microscopy (AFM) presents a powerful tool to measure the cellular stiffness of live human MSCs through appropriate biological sample preparation.

Using AFM, we can obtain three-dimensional images of these samples at the nanometer scale and calculate the Young's modulus, a parameter reflecting the cell's stiffness. By employing a conical silicon tip cantilever with a spring constant of $k = 0.03$ N/m, we can measure the average Young's modulus of the MSCs [29]. Some researches were done on nanomaterials. Mazzini et al .exhibited nano-mechanical properties and average Young's modulus of internal limiting membrane under ocriplasmin treatment by the AFM. They determined the nano-mechanical properties a kind of membrane via treat a type of syndrome with call ocriplasmin. They understood a time-dependent increase of the Young's modulus over time of about 19% of its value in 30 min, up to reach a maximum value [30]. This research produced bio-nanocomposite films for wound dressing applications using gellan gum (GG) and titanium dioxide nanotubes (TiO_2-NTs) via the evaporative casting method. The authors investigated the mechanical properties, antibacterial activity, and chemical interactions between TiO_2-NTs and GG. Their results indicate that incorporating TiO2-NTs improves the mechanical properties of the GG films due to their uniform dispersion within the matrix. While increasing the concentration of TiO_2-NTs reduces water uptake and swelling, it also increases the tensile modulus of the films. This suggests that the films maintain adequate moisture content while diminishing dehydration risks associated with TiO_2-NTs alone. Furthermore, the study found that wounds treated with the GG+TiO_2-NTs films healed faster compared to untreated wounds. The tensile strength and Young's modulus of the films were measured as (4.56 ± 0.15) MPa and (68 ± 1.63) MPa, respectively.

[31]. Also, some investigations done on polymers and biologic systems. Over the past decades, polypyrrole as one of the popular types of conductive polymers (CPs) are used for tissue engineering and drug delivery application [32-35]. In research, polypyrrole nanoparticles (PPy–NPs) conjugated with conductive polymer of PCL (poly (ε-caprolactone) as an aliphatic polyester scaffold with good mechanical property for fabricating biocompatible scaffolds was investigated. PCL scaffolds show poor cell adhesion, migration, and proliferation, low hydrophilicity; and specifically, nothing conductive property. PCL/PPy conductive scaffold was applied in physical, mechanical, and biological fields. They used AFM for determining PCL/PPy composite roughness and mechanical parameters, and indicated that surface roughness of PCL/PPy composite was

increased and Young's Modulus (2 to 4-folds) and tensile strength (3 to 4-folds) as mechanical strength parameters improved.

They showed that surface roughness improvement was depended to PPy–NPs concentration in the PCL/PPy composite scaffolds. Moreover, cell adhesion, growth, and proliferation were related to surface roughness [36].

Moreover, Metabolism and physiological activities of cells can probe by deformability as an inherent property. The erythrocyte deformability shows that it has a strong relation with erythrocyte aging. AFM by a V-shaped silicon nitride cantilever with nominal spring constant of 0.06 N/m have been used. By approaching the tip to the cell, passive and active deformation can be considered. At the first, cell with zero force and from zero force to the separation of the tip - cell are referred as the cell passive deformation and cell active deformation, respectively.

The erythrocytes had the maximum amounts of Young's modulus for active deformation but the minimum amounts for passive deformation. So, the Young's modulus of erythrocytes is calculated as main mechanical specification for determination cell stiffness as a novel biomechanical characteristic for the controlling of aged erythrocytes. The average Young's modulus was determined 1.27 kPa and 1.21 kPa at the center and the terminal radius, over the erythrocyte surface, respectively [37].

Tang et al. identified the significance of passive and active deformations on the mechanical responses of erythrocytes, analyzing them through energy states. The energy consumed during these deformations varied depending on the erythrocyte age, with active deformation energy seen as a crucial mechanical parameter for clearing and removing aged cells. Wounds, whether on the skin or other tissues, represent a major health concern. Such injuries can damage the skin layer and compromise its protective system, potentially leading to infection, bleeding, sepsis, keloids, and scar formation. Therefore, the mechanical properties and antibacterial activity of wound dressings are crucial for proper wound care.

Several metals, including silver, gold, copper, and titanium, have been used to improve the treatment of human cell diseases and wounds [38].

In a study, myricetin (MCE) and its glycoside myricitrin (MCI) flavonols (molecules that have interesting biological activity) are selected and the effect of interactions between 1,2-dimyristoyl-sn-glycero-3- phosphocholine (DMPC) bilayers and these flavonols via simulation study investigated. Flavonols as an important part of human nutrition are a polyphenol, with hydrophilicity and/or hydrophobicity properties, which can affect on various cell membrane parameters such as fluidity via changing membrane enzyme activities and permeability [39]. Their obtained results showed that the interaction between cell membranes and MCI flavonol is more powerful than for MCE flavonol. It can be attributed to the difference in polarities between MCE and MCI [40].

Damaged tissues can treat via biological performances including 3D artificial matrices or scaffolds. This is nominated as tissue engineering (TE) [41]. These scaffolds should be built from materials with open porosity (controllable shape and size of pores) and biocompatible. Stiffness and permeability of the scaffold is significant in TE. In this regard, AFM was applied to measure mechanical properties of various diameters of poly (ε-caprolactone) (PCL) fibers in the macro and nanoscale. Also, Young's modulus values were determined using force-distance curves by AFM. Their results showed that changes in fiber diameters can have influence on the mechanical properties scaffolds as a significant factor in 3D-printed fibers designing [42].

Cancer is a serious problem among diseases and it is considered as a significant challenge in new researches. It is reported that tumor can start from likely a single cell within a cluster of precancerous cells that contribute oncogenetic transformation [43]. Furthermore, cell mechanical properties involving of tissue formation, cell functionality, stem cell differentiation are significant factors in cancer diagnosing. In this regards, atomic force microscope can apply for studding cell mechanics, pericellular coat or brush-like layer surrounding eukaryotic [44]. Atomic Force Microscopy (AFM) holds promise for enhancing our understanding of factors responsible for cancer initiation. A study used AFM to investigate the physical properties of cancer-initiating cells and surrounding tissues in three animal tumors. Identifying these factors could impact cancer onset and progression.

The study revealed a significant increase in the effective Young's modulus of surrounding tissues compared to cancer-initiating cells, indicating that surrounding tissues were stiffer. Notably, cancer-initiating cells exhibited softer properties than advanced cancer cells. These AFM analyses of cell physical parameters demonstrated crucial changes associated with cancer development.

AFM indentation was employed to examine cancer-initiating cells and surrounding tissues as controls. Statistically significant differences were observed in the mechanical properties and effective Young's modulus between these groups. Importantly, cancer-initiating cells displayed a decrease in effective Young's modulus compared to surrounding tissues [45].

In research, the properties of collagen fibrils are studied using AFM. Tendon tensile strength and many other connective tissues are created via Collagen fibrils. Collagen fibrils with protein structures are rope-like supermolecular and its hierarchical structures are held together via intermolecular and covalent bonding between single molecules. For study of single collagen fibrils from tendons, atomic force microscopy with high resolution and velocity, and hydrated mechanical mapping technique had been used.

They separated five fibrils of each tendon from five individual animals (a total 25 fibrils), and they had mechanically investigated fibrils from tendons as hydrated and dehydrated. Each fibril was imaged using AFM in the dehydrated and rehydrated states. The fibril deformation at a point was described from the force/distance curve. They showed that all fibrils demonstrated microscale variation and the distribution of these variations along the fibril length were calculated. They proposed that the source of this variation in modulus is local differences in the collagen molecules number per unit length and/or differences in crosslink density [46].

A study measured the nanoscale effects of various soft drinks on human teeth enamel using Atomic Force Microscopy (AFM). The study focused on roughness (Rq) and elastic modulus (E) changes over time by floating teeth in different beverages. By calculating topography and elastic modulus, researchers aimed to identify early signs of enamel weakening, a crucial step in understanding dental erosion. Dental erosion results from acidic foods and drinks, medication, and certain treatments. It removes hard dental tissue, leaving the enamel roughened and weakened. This erosion allows bacteria and acids to penetrate the tooth's structure, reaching the dentin and causing sensitivity to heat, cold, sweet, and sour foods. This can even lead to hypersensitivity.

The study's findings highlight the importance of elastic modulus as a key factor in detecting the initial stages of enamel weakening during the etching process [47].

AFM strongly can help to identify mechanical and structural differences in each cell type [48,49]. Ngayama et al. studied macroscopic and microscopic analysis of the mechanical properties, adhesion force and cell-substrate adhesion strength of different cell types via AFM analysis.

According to their results, the mechanical properties of vascular smooth muscle cells (VSMCs) were up two times larger than those of HeLa cells. It is attributed to the internal tension and shape discipline of the actin cytoskeleton [50].

Three dimensional biocompatible materials with sizes micro to nanoscale can be used for bone formation process or neural tissue reconstruction, because they are sensitive to the mechanical properties of the substrates. In research, Buchroithner et al. studied mechanical properties of biocompatible materials by AFM. They measured two biocompatible resins (pentaerythritol triacrylate (PETA) and hybrid OrmoComp monomers) Young's modulus and compared to two resins which are commonly used in Multiphoton lithography. Young's modulus value is reported in the range of 100 Mpa. They indicated that OrmoComp Young's modulus was the smallest which it is attributed to a its high aspect ratio [51].

In the worldwide, one of the deadliest diseases is tumor in glioblastoma (GBM). Hohman et al. studied the effect of Metastasis-associated in colon cancer 1 (MACC1), which it can increases the migration speed of single cells and their elastic modulus, that cause the decreased adhesion and increased elasticity. At first, Cells were permitted to adhere to a petri dish and after the starting the test, single cells were investigated using AFM tip for identifying the Young's modulus. Moreover, the average diameter of the cell was measured, that giving a good estimate of the initial cell-cell distance. The changes are seen in adhesion, elasticity and tension, which it leads to inhibited GBM cell migration and thus improvement of disease [52].

Application of AFM in the Young's modulus determination in the unbiological science

Some investigations were done on nano materials. Short fiber reinforced rubber composites have significant properties, which they can applied for diverse industrial applications. The interfacial interaction and interfacial nanomechanical properties between fibers and rubber can affect on interface quality as a key factor for the increasing of efficiency, the mechanical properties and failure behavior of the composites. Tian et al. studied interfacial interaction of three kinds fibrillar silicate/elastomer nanocomposites (FS/NR) by combination of quantitative nanomechanical technique and atomic force microscopy (AFM-QNM). These nanocomposites exhibited excellent performance, which their mechanical properties and Young's modulus were quantitatively determined via AFM-QNM. Interfacial thickness and Young's modulus of the modified FS/NR composites were higher than unmodified-FS/NR composites. This could be ascribed to presence of chemical bonds and physical entanglement between modified-FS and NR matrix and between unmodified-FS and NR matrix, respectively. This research can provide to deep comprehend the interface of nanofiber reinforced composites, and it can help to design of interfacial high performance rubber composites [53]. Hyperbranched polyglycerols (hbPGs) are highly biocompatible materials due to their high molecular weight. Various analytical techniques were used to characterize the synthesized materials, which have also been explored for drug delivery applications [54-55]. Atomic Force Microscopy (AFM) offers a powerful tool to measure the Young's modulus, adhesion force in molecular bonds, and surface chemical state of hbPGs, making them an attractive polymer for drug delivery. A study reported that the Young's modulus of hbPGs strongly increased when deposited on a mica substrate, which was attributed to the formation of intramolecular hydrogen bonds [56].

Textile wastewater often contains dyes and other chemicals that need to be removed before discharge to protect the environment. Membrane technology, including ultrafiltration (UF) and nanofiltration (NF), is a promising approach for this purpose due to its economic viability, high removal efficiency, and minimal environmental impact. However, these membranes can suffer from fouling, reducing their effectiveness. Modifying the membranes with nanoparticles presents a new way to improve their surface properties and mitigate fouling. Sakarkar et al. investigated the use of six different polyvinyl alcohol (PVA)/titanium dioxide (TiO2) composite membranes coated on polyvinylidene fluoride (PVDF) for dye removal from textile wastewater using the dip-coating method. They compared the mechanical properties of these composite membranes. Their results showed that the root mean square roughness of the pure PVDF membrane was 1.067 nm, while the composite membrane containing 12 wt% PVA displayed a significantly higher roughness of 120 nm [57].

Moreover, using the SEM, AFM, FTIR, XRD and contact angle results, the interactions between TiO_2 nanoparticles and PVA in the coating were detected, which led to changed surface morphologies and increased hydrophilicity of the membranes [57].

Some researches were done on polymers and unbiologic science. Fang et al. studied the Young's modulus of the membranes of Natural oil bodies (OBs) such as soybean, sesame, and peanut via AFM. They showed that membrane structure and surface molecular conformation can lead to differ between the mechanical properties of the various OBs. Higher protein/oil ratio in Obs can provide smaller size, stronger mechanical traits with more stability, that these properties are benefit in the membrane in industrial applications [58].

Diamond-like carbon (DLC) films, valuable for their semiconducting properties, were successfully deposited on Si substrates using helicon wave plasma chemical vapor deposition (HW-PCVD) with Ar/CH_4 mixtures at room temperature. These films exhibit high biocompatibility, hardness, chemical resistance, electrical resistivity, and low friction coefficients, making them suitable for various electronic applications.

The influence of CH_4 flow rate (ranging from 5 to 25 sccm) on the surface energy of the DLC films was investigated using Atomic Force Microscopy (AFM). It was found that the films achieved the highest Young's modulus of 11 GPa at a CH_4 flow rate of 25 sccm, attributed to the presence of C-C sp^3 bonds. Interestingly, the AFM study also revealed that the DLC film surfaces were relatively soft [59].

In fact, by increasing the PVA value, tensile strength and Young's modulus of the coated membranes were increased, due to agglomeration of the TiO_2 nanoparticles in the composite which can increase the roughness. In addition, dye removal has been more common for high molecular weight dye molecules because they are trapped in small membrane pores.

The valorization of naturally resources can help solve environmental problems caused by the excessive use of fossil resources. Lignin containing cellulose nanofibers (LCNFs) as lignocellulosic resources can considered as a suitable option for using in the composites, biomedical devices, filtration and packaging applications. Yang et al. produced LCNFs through wheat residues and then it was inserted into a polyvinyl alcohol (PVA) matrix. The introduce of LCNFs in the PVA composites films, resulted in significant improvements in tensile Strength, Young's modulus, thermal resistance, surface properties and slight decrease in elongation at break. So, LCNFs are expected to be a good candidate for various applications, including as additives to composites, biomedical devices and so on [60].

Glass molding is an effective and green environmental method to make the optical elements such as aspheric lenses. Optical elements are fabricated by various coating including metal or nitride on various surfaces for glass molding applications [61-62]. A previous study by Li et al. investigated the effect of CrxWyNz coatings on cemented carbide (WC-8Co) under thermal-mechanical cycles in a nitrogen atmosphere. CrxWyNz coatings were deposited on WC-8Co using plasma-enhanced magnetron sputtering (PEMS) technology and then evaluated for their performance in a precision glass molding machine (PGMM). Atomic Force Microscopy (AFM) was employed to determine the mechanical properties of the coated surfaces.

The study found that increasing the W content in the CrxWyNz coatings led to a simultaneous increase in Young's modulus and decrease in surface roughness. Additionally, the coatings offered protection against oxidation reactions during the thermal-mechanical cycles, resulting in reduced surface roughness in the contact area compared to the non-contact area. Overall, the study concluded that CrxWyNz coatings (with $18 \leq x \leq 27$ and $24 \leq y \leq 28$) represent a suitable protective coating for this application [63].

Mechanical properties of titanium carbon nitride (TiCN) coatings were investigated by some researchers in the past few years, because TiCN have higher hardness than commercial TiAlN and TiN coatings [64]. Das et al. synthesized TiCN thin films on Si substrate by CVD technique under different N_2 gas flow rate (6-15 sccm) and evaluated the performance of CVD method for the growth of TiCN coating over machine apparatus at high temperatures. Various analysis was done for identifying of morphological, structural, corrosion behavior and mechanical properties of the coatings. AFM analysis was used for determination of surface roughness. Results indicated that by increasing of N_2 flow rate, Hardness (H) and Young's modulus (E) and particle size were increased. The nanoindentation result detected an increase in coating hardness and Young's modulus by an increase in N_2 flow rate in the range of 23.85±1.87 to 27.88±1.86 sccm and 449.65 to 486.22 sccm, respectively. Increased N_2 flow rate gained in the decreased coatings roughness.

Maximum surface roughness and Young's modulus was reported as 48.25 nm and 486.22 Gpa in low and high flow rate, respectively [65].

Conclusion

Atomic force microscopy (AFM) has emerged as a powerful technique in both scientific and industrial fields, enabling the study of various physical and structural properties of compounds at the nanoscale. One key strength of AFM is nano-indentation, which allows for accurate measurement of Young's modulus, providing valuable quantitative information about the mechanical properties and nature of materials. This rapidly growing field of knowledge holds immense potential for a deeper understanding of mechanical characteristics at the molecular and atomic scales. Beyond its impressive mechanical characterization capabilities, AFM's ease of use and non-destructive nature have cemented its position as a critical tool in biology and surface science research. Furthermore, its versatility across diverse applications, combined with its exceptional nanoscale resolution, makes AFM an increasingly popular choice in both research and industrial settings.

References

[1] Panitz, J. S. P., Desenvolvimento e implementação de metodologias para a determinação da deformabilidade e tensões em maciços gn´aissicos, Pontif´ıcia Universidade Cat´olica Do Rio De Janeiro. Rio de Janeiro, Brazil. IJM, P. 2007; 11: 1096-1109.

[2] Bezerra, M. T. P. A., Silva, F. M., de Souza Soares, M. M. N., Relações do mo´dulo de elasticidade dinaˆmico, esta´tico e resisteˆncia a` compressão do concreto. Anais do 51° Congresso Brasileiro do Concreto–IBRACON. J. Augusto Cesar da Silva. 2009; 20: 1-10.

[3] Chang, Y. R., Raghunathan, V. K., Garland, S. P., Morgan, J. T., Russel, P., Murphy, C. J., Automated AFM force curve analysis for determining elastic modulus of biomaterials and biological samples. J. Mech. Behav. Biomed. Mater. 2014; 37: 209–218.

[4] Putman, C. A. J., Van der Werf K. O., De Grooth B. G., Van Hulst N. F., Greve J., Tapping mode atomic force microscopy in liquid. J. Appl. Phys. Lett. 1994; 64: 2454.

[5] Weymouth, A. J., Wastl, D., Giessibl, F. J., Advances in AFM: seeing atoms in ambient conditions. e-J. Surf. Sci. Nanotech. 2018; 16: 351–355.

[6] M. Hua, Y., Y. Han, C., Y. Shiuan, L., O. Sheng, L., Alteration of Young's modulus in mesenchymal stromal cells during osteogenesis measured by atomic force microscopy. B. B. R. C. 2020; 526: 827-832.

[7] Fuzhou, T., Dong, C., Shichao, Z., Wenhui, H., Jin, C., Houming, Z., Zhu, Z., Xiang, W., Elastic hysteresis loop acts as cell deformability in erythrocyte aging. J. BBA – Biomembranes. 2020; 1862: 183309.

[8] Majewskaa, M., Mrdenovica, D., Pietaa, I.S., Nowakowskia, R., Pietaa, P., Nanomechanical characterization of single phospholipid bilayer in ripple phase with PF-QNM AFM. BBA – Biomembranes. 2020; 1826: 183-347.

[9] Hermanowicz, P., Determination of Young's modulus of samples of arbitrary thickness from force distance curves: numerical investigations and simple approximate formulae, International Journal of Mechanical Sciences, 2020.

[10] Zee Ma, Y., Janz, R., Glossary for Unconventional Oil and Gas Resource Evaluation and Development. In Unconventional Oil and Gas Resources Handbook. 2016.

[11] Sirohi, R. S. A., Course of Experiments with He-Ne laser. Wiley Eastern Limited, New Delhi. 1986; 67.

[12] Sadegh Hassani, S., Afzali, J., Khosravi, M., Atomic force microscopy. Gisoom publisher Aug. 2014.

[13] Sobat, Z., Sadegh Hassani, S., An overview of scanning near field optical microscopy in characterization of nanomaterials. Int. J. Nano. Dim. 2014; 5: 203-308.

[14] Sadegh Hassani, S., Scanning tunneling microscopy and its application under electrochemical conditions. J. RIPI Publisher. 2011; 2.

[15] Sadegh Hassani, S., Daraee, M., Sobat, Z., Application of atomic force microscopy in adhesion force measurements. J. Adhes Sci Technol. 2021; 35: 221-241.

[16] Kaman, J., Young's Modulus and Energy Dissipation Determination Methods by AFM, with Particular Reference to a Chalcogenide Thin Film, Periodica Polytechnica Electrical Engineering and Computer Science, 2015, 59(1).

[17] Sadegh Hassani, S., Sobat, Z., Aghabozorg, H. R., Scanning probe lithography as a tool for studying of various surfaces. NSNTAIJ. 2008; 2: 94-98.

[18] Sadegh Hassani, S., Aghabozorg, H. R., Recent Advances in Nanofabrication Techniques and Applications. Chapter title: Nanolithography Study Using Scanning Probe Microscope. InTech publisher. 2011.

[19] Tick Boon Loh, Yutong Wu, Siang Huat Goh, Kian Hau Kong, Kheng Lim Goh and Jun Jie Chong, Jun Jie Chong, An Integrated Approach for the Determination of Young's Modulus of a Cantilever Beam Using Finite Element Analysis and the Digital Image Correlation (DIC) Technique, *Electronics* 2022, *11*(18), 2826.

[20] Roa, J. J. , Oncins, G., Diaz, J., Sanz, F., Segarra, M., Calculation of Young's Modulus Value by Means of AFM. J. Recent Pat Nanotechnol. 2011; 5: 27-36.

[21] J. Price, W., A. Leigh, S., M. Hsu, S., E. Patten, T., Liu, G. Y., Measuring the Size Dependence of Young's Modulus Using Force Modulation Atomic Force Microscopy. J. Phys. Chem. A. 2006; 110: 1382-1388.

[22] I. Krymskaya, K., V. Andreeva, N., V.Filimonov, A., A technique for determining Young's modulus of biological objects using atomic-force microscopy in the wide temperature range below Rt. 2016; 2: 217-223.

[23] Maugis, D., Barquins, M., Adhesive contact of sectionally smooth ended punches on elastic half space theory and experiment. J. Phys. D. Appl. Phys. 1983; 16: 1843.

[24] Li, M., Xi, N., Wang, Y., Advances in atomic force microscopy for single-cell analysis, J. Nano Res. 2019; 12: 703-718.

[25] N. Patel, A., Kranz, C., (Multi) functional Atomic Force Microscopy Imaging. in Annual Review of Analytical Chemistry. Annual Review of Analytical Chemistry. J. Palo Alto: Annual Reviews. 2018; 11:329-350.

[26] Yunkyung, L., Manhee, L., Sangmin, A., Sang-Joon, C., Quantitative Visualization of the Nanomechanical Young's Modulus of Soft Materials by Atomic Force Microscopy Seongoh Kim. Nanomaterials. 2021; 11: 1593.

[27] Yuta, N., Yukihiro, Y., Yuki, H., Yoshitaka, N., Method for measuring Young's modulus of cells using a cell compression microdevice Tairo Yokokura. Int J Eng Sci. 2017; 114: 41-48.

[28] K. Dimitriadis, E., Horkay, F., Maresca, J., Kachar, B., S. Chadwick, R., Determination of Elastic Moduli of Thin Layers of Soft Material Using the Atomic Force Microscope. Biophys. J. 2002; 82: 2798–2810.

[29] M. Hua, Y., Y. Han, C., Y. Shiuan, L., O. Sheng, L,. Alteration of Young's modulus in mesenchymal stromal cells during osteogenesis measured by atomic force microscopy. B. B. R. C. 2020; 526: 827-832.

[30] Mazzini, A., Palermo, F., Pagliei, V., Romano, S., Papi, M., Zimatore, G., Falsini, B., Rizzo, S., D. Spirito, M., Ciasca, G., M. Minnella, A., A time-dependent study of nano-mechanical and ultrastructural properties of internal limiting membrane under ocriplasmin treatment. J. Mech Behav Biomed Mater. 2020; 110: 103853.

[31] M. Hasmizam, R., N. Afrifah, I., K. A. Mat, A., Titanium dioxide nanotubes incorporated gellan gum bio-nanocomposite film for wound healing: Effect of TiO2 nanotubes concentration. Int. J. Biol. Macromol. 2020; 153: 1117-1135.

[32] Xiangru, F., Jiannan, L., Xi, Z., Tongjun, L., Jianxun, D., Xuesi, C., Electrospun polymer micro/nanofibers as pharmaceutical repositories for healthcare, J. Control. Release. 2019; 302: 19–41.

[33] T. I, H., J. I, K., M. Kumar, J., C. Hee, P., C. Sang, K., Simultaneous regeneration of calcium lactate and cellulose into PCL nanofiber for biomedical application, J. Carbohydr. Polym. 2019; 212: 21–29.

[34] P. Bhattarai, P., P. Tiwari, A., Maharjan, B., Tumurbaatar, B., H. Park, C., S. Kim, C., Sacrificial template-based synthetic approach of polypyrrole hollow fibers for photothermal therapy. J. Colloid Interface Sci. 2019; 534: 447–458.

[35] T. Hai, L., Yukyung, K., Hyeonseok, Y., Electrical and Electrochemical Properties of Conducting Polymers. J. Polym. 2017; 9: 9040150.

[36] Maharjan, B., K. Kaliannagounder, V., S. Rim, J., G. Prasad. A., D. Prasad, B., Ghizlane, C., H. Park, C., C. Sang. K., In-situ polymerized polypyrrole nanoparticles immobilized poly(ε-caprolactone) electrospun conductive scaffolds for bone tissue engineering. J. Mater. Sci. Eng. C. 2020; 114: 111056.

[37] Fuzhou, T., Dong, C., Shichao, Z., Wenhui, H., Jin, C., Houming, Z., Zhu, Z., Xiang, W., Elastic hysteresis loop acts as cell deformability in erythrocyte aging. J. BBA – Biomembranes. 2020; 1862: 183309.

[38] V. Giang, N., Hoang, T., D. Huynh, M., H. Trung, T., D. Lam, T., M. T, Vu., Effect of titanium dioxide on the properties of polyethylene/TiO_2 nanocomposites. J. Compos. B. 2013; 45: 1192–1198.

[39] Selvaraj, S., Krishnaswamy, S., Devashya, V., Sethuraman, S., M. Krishnan, U., Influence of membrane lipid composition on flavonoid–membrane interactions: implications on their biological activity, J. Prog. Lipid Res. 2015; 58: 1–13.

[40] Sadžak, A., Brkljača, Z., Crnolatac, I., Baranović, G., Šegota, S., Flavonol clustering in model lipid membranes: DSC, AFM, force spectroscopy and MD simulations study, J. Colloids and Surfaces B: Biointerfaces. 2020; 193: 111147.

[41] Idaszek, J., Kijeńska, E., Łojkowski, M., Swieszkowski, W., How important are scaffolds and their surface properties in regenerative medicine, J. Appl. Surf. Sci. 2016; 388: 762–774.

[42] Gorecka, Z., Idaszek, J., Kołbuk, D., Choińska, E., Chlanda, A., Święszkowski, W., The effect of diameter of fibre on formation of hydrogen bonds and mechanical properties of 3D-printed PCL. Mater. Sci. Eng. C. 2020; 114: 111072.

[43] Sokolov, I., Dokukin, M. E., Kalaparthi, V., Miljkovic, M., Wang, A., Seigne, J. D., Grivas, P., Demidenko, E., Noninvasive diagnostic imaging using machine-learning analysis of nanoresolution images of cell surfaces: detection of bladder cancer. J. Proc. Natl. Acad. Sci. U.S.A. 2018; 115: 12920–12925.

[44] Wu, P. H., R. B. Aroush, D., Asnacios, A., Chen, W. C., E. Dokukin, M., L. Doss, B., D. Smet, P., Ekpenyong, A., Guck, J., V. Guz, N., A. Janmey, P., S. H. Lee, J., M. Moore, N., Ott, A., Poh, Y. C., Ros, R., Sander, M., Sokolov, I., R. Staunton, J., Wang, N., Whyte, G., Wirtz, D., A comparison of methods to assess cell mechanical properties. J. Nat. Methods 15. 2018; 491–498.

[45] Makarova, N., Vivek, K., Andrew, W., Chris, W., Dokukin, M. E., K. Kaufman, C., Zon, L., Sokolov, I., Difference in biophysical properties of cancer-initiating cells in melanoma mutated zebrafish. J. Mech Behav Biomed Mater. 2020; 107: 103746.

[46] J. Baldwin, S., Sampson, J., J. Peacock, C., L. Martin, M., P. Veres, S., Lee, J. M., Kreplak, L., A new longitudinal variation in the structure of collagen fibrils and its relationship to locations of mechanical damage susceptibility. J. Mech Behav Biomed Mater. 2020; 110: 103849.

[47] Panpan, Li., Chungik, O., Hongjun, K., Melodie, C. G., Gun, P., Albina, J., Jiwon, Y., Hoon, K., Jeongjae, R., Seungbum, H., Nanoscale effects of beverages on enamel surface of human teeth: An atomic force microscopy study. J. Mech Behav Biomed Mater. 2020; 110: 103930.

[48] Urbanska, M., Winzi, M., Neumann, K., Abuhattum, S., Rosendahl, P., Müller, P., Taubenberger, A., Anastassiadis, K., Guck, J., Single-cell mechanical phenotype is an intrinsic marker of reprogramming and differentiation along the mouse neural lineage. J. Development. 2017; 144: 4313–4321.

[49] Vahabikashi, A., Park, C. Y., Perkumas, K., Zhang, Z., K. Deurloo, E., Wu, H., A. Weitz, D., Stamer, W. D., D. Goldman, R., J. Fredberg, J., Johnson, M., Probe sensitivity to cortical versus intracellular cytoskeletal network stiffness. J. Biophys. 2019; 116: 518–529.

[50] Kazuaki, N., Shigeaki, O., Shota, O., Akiko, S., Macroscopic and microscopic analysis of the mechanical properties and adhesion force of cells using a single cell tensile test and atomic force microscopy: Remarkable differences in cell types. J. Mech Behav Biomed Mater. 2020; 110: 103935.

[51] Buchroithner, B., Hartmann, D., Mayr, S., Oh, Y. J., Sivun, D., Karner, A., Buchegger, B., Griesser, T., Hinterdorfer, P., A. Klarb, T., Jacak, J., 3D multiphoton lithography using biocompatible polymers with specific mechanical properties, J. Nanoscale Adv. 2020; 2: 2422.

[52] Offroy, M., Razafitianamaharavo, A., Beaussart, A., Pagnoutb, C., F. L. Duval, J., Fast automated processing of AFM Peak Force curves to evaluate spatially resolved Young modulus and stiffness of turgescent cells, J. RSC Adv. 2020; 10: 19258.

[53] Chenchen, T., Yuxing, F., Guangyu, C., Yonglai, L., Chunmeng, M., Nanying, N., Liqun, Z., Ming, T., Interfacial nanomechanical properties and chain segment dynamics of fibrillar silicate/elastomer nanocomposites. J. Composites Part B 193. 2020; 108048.

[54] Schön, P., Görlich, M., J. J. Coenen, M., A. Heus, H., Speller, S., Nonspecific protein adsorption at the single molecule level studied by atomic force microscopy, J. Langmuir. 2007; 23: 9921–9923.

[55] Meng, L., Jinjie, Z., Nianwa, T., Hang, S., Jinling, H., Horizontal gene transfer from bacteria and plants to the arbuscular mycorrhizal fungus Rhizophagus irregularis, J. Front. Plant Sci. 2018; 9: 701.

[56] Haigang, W., Qunzhi, C., Mingzhu, J., Xue, X., Xueyan, L., Nan, H., Ke, L., Jinlong, Y., Bingyang, S., Evaluation of nanomechanical properties of hyperbranched polyglycerols as prospective cell membrane engineering block, J. Colloids and Surfaces B: Biointerfaces. 2020; 190: 110968.

[57] Sakarkar, S., Muthukumaran, S., Jegatheesan, V., Evaluation of polyvinyl alcohol (PVA) loading in the PVA/titanium dioxide (TiO2) thin film coating on polyvinylidene fluoride (PVDF) membrane for the removal of textile dyes, J. Chemosphere. 2020; 257: 127144.

[58] Yang, N., Su, C., Zhang, Y., Jia, J., L. Leheny, R., Nishinari, K., Fang, Y., O. Philips, G., In situ nanomechanical properties of natural oil bodies studied using atomic force microscopy. J. Colloid Interface Sci. 2020; 570: 362–374.

[59] Jia-li, C., Pei-yu, J., Yan, Y., C. Gang, J., L. Jian, Z., X. Mei, W., The structure and properties of amorphous diamond-like carbon films deposited by helicon wave plasma chemical vapor deposition. J. Thin Solid Films. 2020; 709: 138167.

[60] Mingyan, Y., Xiao, Z., Shuyi, G., Yan, D., Xiaofeng, G., Preparation of lignin containing cellulose nanofibers and its application in PVA nanocomposite films. Int. J. Biol. Macromol. 2020; 158: 1259–1267.

[61] S. Hong, L., I. Hwan, K., T. Youn, K., Surface failure analysis of AlCrN coating on WC substrate subjected to high-temperature oxidation in glass-molding machine, J. Appl. Surf. Sci. 2018; 405: 210–216.

[62] X. Yan, Z., J. Jun, W., L. Xian, C., J. Long, L., L. Fu, H., C. Ming, L., Yong, Z., Anti-sticking Re-Ir coating for glass molding process, J. Thin Solid Films. 2015; 584: 305–309.

[63] Kangsen, L., Gang, X., Xinfang, H., Qiang, C., Zhiwen, X., Feng, G., Surface evolution analysis of CrxWyNz coatings on WC mold in glass molding Process. J. Surf. Coat. Technol. 2020; 393: 125839.

[64] Bull, S. J., Bhat, D. G., Staia, M. H., Properties and performance of commercial TiCN coatings Part 1: coating architecture and hardness modelling, J. Surf. Coat. Technol. 2003; 163–164: 499–506.

[65] Soham, D., Spandan, G., P. Protim, D., Ranjan, K. G., Analysis of morphological, microstructural, electrochemical and nano mechanical characteristics of TiCN coatings prepared under N_2 gas flow rate by chemical vapour deposition (CVD) process at higher temperature. J. Ceram. Int. 2020; 46: 10292–10298.